





NLRX1 promotes immediate IRF1-directed antiviral responses by limiting dsRNA-activated translational inhibition mediated by PKR

Hui Feng^{1,2}, Erik M Lenarcic^{1,3,8}, Daisuke Yamane^{1,2,7,8}, Eliane Wauthier^{1,4}, Jinyao Mo^{1,2}, Haitao Guo^{1,5}, David R McGivern^{1,2} , Olga González-López^{1,2}, Ichiro Misumi^{1,4} , Lola M Reid^{1,5}, Jason K Whitmire^{1,3,4} , Jenny P-Y Ting^{1,4}, Joseph A Duncan^{1,2,6}, Nathaniel J Moorman^{1,3} & Stanley M Lemon¹⁻³ 

NLRX1 is unique among the nucleotide-binding-domain and leucine-rich-repeat (NLR) proteins in its mitochondrial localization and ability to negatively regulate antiviral innate immunity dependent on the adaptors MAVS and STING. However, some studies have suggested a positive regulatory role for NLRX1 in inducing antiviral responses. We found that NLRX1 exerted opposing regulatory effects on viral activation of the transcription factors IRF1 and IRF3, which might potentially explain such contradictory results. Whereas NLRX1 suppressed MAVS-mediated activation of IRF3, it conversely facilitated virus-induced increases in IRF1 expression and thereby enhanced control of viral infection. NLRX1 had a minimal effect on the transcription of *IRF1* mediated by the transcription factor NF- κ B and regulated the abundance of IRF1 post-transcriptionally by preventing translational shutdown mediated by the double-stranded RNA (dsRNA)-activated kinase PKR and thereby allowed virus-induced increases in the abundance of IRF1 protein.

The NLR family of proteins is recognized for its roles in inflammatory-mediated responses to both pathogen-associated molecular patterns and damage-associated molecular patterns¹. However, several NLR proteins, including NLRX1, NLRC3, NLRC5 and NLRP12, act as negative regulators of innate immunity with the ability to check type I interferon responses or NF- κ B-induced pro-inflammatory cytokines²⁻⁵. NLRX1 is distinguished from other members of the NLR family by its localization to mitochondria, where it interacts with MAVS through its unique amino-terminal X domain and nucleotide-binding-oligomerization domain, sequesters MAVS and suppresses virus-induced interferon responses mediated by the pathogen sensor RIG-I⁶. NLRX1 also negatively regulates lipopolysaccharide-induced activation of NF- κ B, interacting with the adaptor TRAF6 in unstimulated cells and being recruited to the NEMO-IKK signaling complex following lipopolysaccharide stimulation via its leucine-rich-repeat domain³. Deletion or functional knockdown of NLRX1 results in heightened interferon responses to the synthetic RNA duplex and Toll-like receptor 3 (TLR3) agonist poly(I:C) or RNA viruses, as well as increased inflammatory responses^{3,6,7}. Acting like a Swiss Army knife, NLRX1 also interacts with STING through its nucleotide-binding-oligomerization domain and thereby inhibits interferon

responses to DNA viruses mediated through the cGAS-cGAMP signaling pathway⁸. Abundant evidence thus supports the concept that NLRX1 functions as a checkpoint inhibitor of early innate immune responses to both DNA viruses and RNA viruses.

However, not all studies have shown that NLRX1 exerts negative regulatory effects on innate immune responses to viruses. Sendai virus (SeV)-induced RIG-I- and MAVS-dependent phosphorylation of IRF3 and production of interferon- β (IFN- β) and the chemokine IP10 (CXCL10) are reported to be unchanged in *Nlrp12*^{-/-} mouse embryonic fibroblasts (MEFs), relative to that of wild-type MEFs, as are cytokine IL-6 and IFN- β responses to poly(I:C)⁹. Although inflammatory responses to infection with influenza virus are enhanced in the lungs of *Nlrp12*^{-/-} mice relative to those in the lungs of wild-type mice⁷, their macrophage-mediated interferon responses are impaired, secondary to enhanced apoptosis¹⁰. Also, rather than inhibiting NF- κ B signaling, overexpression of NLRX1 enhances such signaling by amplifying the production of reactive oxygen species in response to several stimuli¹¹. Such findings are puzzling given that the preponderance of evidence favors a negative regulatory role for NLRX1. While they might reflect different experimental conditions, they have fueled controversy about the regulatory role of NLRX1.

¹Lineberger Comprehensive Cancer Center, The University of North Carolina at Chapel Hill, Chapel Hill, North Carolina, USA. ²Department of Medicine, The University of North Carolina at Chapel Hill, Chapel Hill, North Carolina, USA. ³Department of Microbiology & Immunology, The University of North Carolina at Chapel Hill, Chapel Hill, North Carolina, USA. ⁴Department of Genetics, The University of North Carolina at Chapel Hill, Chapel Hill, North Carolina, USA. ⁵Department of Cell Biology and Physiology, The University of North Carolina at Chapel Hill, Chapel Hill, North Carolina, USA. ⁶Department of Pharmacology, The University of North Carolina, Chapel Hill, North Carolina, USA. ⁷Present address: Department of Microbiology and Cell Biology, Tokyo Metropolitan Institute of Medical Science, Setagaya-ku, Tokyo, Japan. ⁸These authors contributed equally to this work. Correspondence should be addressed to S.M.L. (smlmemon@med.unc.edu).

Here we sought to understand how NLRX1 influences innate immune responses to viral infection of human hepatocytes. Hepatocytes are targeted for infection by several medically important viruses, including hepatitis A virus (HAV) and hepatitis C virus (HCV), which are RNA viruses that cause inflammatory diseases of the liver¹². We found that NLRX1 competed with dsRNA-activated PKR for binding to viral RNA and that it promoted early innate immune antiviral responses by protecting NF- κ B-driven increases in the expression of IRF1 from translational suppression mediated by PKR. Hepatocytes deficient in NLRX1 expression had diminished accumulation of IRF1 but more formation of IRF3 dimers in response to viral infection, relative to that of hepatocytes sufficient in NLRX1; this revealed opposing actions of NLRX1 on key signaling pathways. Our data identify a previously unknown and sophisticated regulation of early innate immune responses by NLRX1 that, overall, promotes immediate antiviral defense in hepatocytes.

RESULTS

NLRX1 is a positive immunoregulator in hepatocytes

To determine how NLRX1 influences antiviral responses in hepatocytes, we used CRISPR-Cas9 gene editing to eliminate its expression in PH5CH8 cells, which are T antigen-transformed primary human hepatocytes with functional signaling via RIG-I and TLR3 (refs. 13,14). NLRX1 expression was detected in PH5CH8 cells transduced with a nontargeting single guide RNA (sgRNA) with a scrambled sequence (called 'control PH5CH8 cells' throughout) but not in either of two independent PH5CH8 cell lines (NLRX1-T2 and NLRX1-T3) transduced with different *NLRX1*-specific sgRNAs (Fig. 1a and Supplementary Table 1). We initiated HCV replication in these cells by electroporating synthetic viral RNA and the duplex microRNA miR-122, an essential HCV host factor that PH5CH8 cells lack¹⁵, together into the cells. We demonstrated that subsequent increases in viral RNA were due to true viral replication because they were blocked by a direct-acting antiviral inhibitor (Fig. 1b). We also infected the cells directly with HAV¹⁶. Replication of each virus was enhanced in NLRX1-deficient (NLRX1-T2 and NLRX1-T3) cells relative to that of control PH5CH8 cells (Fig. 1b). We similarly assessed HAV replication in primary human fetal hepatoblasts (HFHs). Partial depletion of NLRX1 via RNA-mediated interference boosted viral replication in cells from two donors (Fig. 1c), which confirmed an antiviral role for NLRX1 in human liver cells.

Although innate immune responses restrict infection with HAV or HCV in PH5CH8 cells, it is difficult to document the induction of antiviral cytokines in these cells following viral challenge. We thus employed a classic agonist of RIG-I signaling, SeV, to define the effect of NLRX1 deficiency on cytokine responses. We observed significantly lower *IFNB1*, *IFNL1*, *IL1B* and *IL6* mRNA responses early (at 3 h) in SeV-infected NLRX1-deficient (NLRX1-T2 and NLRX1-T3) cells than in SeV-infected control PH5CH8 cells (Fig. 1d). This effect was no longer evident at 8 h, by which time these responses had substantially subsided (Supplementary Fig. 1a). NLRX1 deficiency also impaired the accumulation of *IL1B* and *IL6* mRNA, but not that of *IFNB1* mRNA, in response to poly(I:C) added to the medium (Fig. 1e). NLRX1 deficiency consistently reduced the amount of IL-6 protein induced in response to stimulation with SeV or poly(I:C) (Fig. 1f). Likewise, small interfering RNA (siRNA)-mediated depletion of NLRX1 significantly impaired the increase in IL-6 protein induced by infection of primary HFHs with SeV (Fig. 1g). Neither HAV nor HCV replicates in mouse cells, but we observed a reduction of approximate fourfold in the early (3-hour) intrahepatic *Irfnb* and *Il6* mRNA responses to synthetic HAV RNA administered

intravenously to *Nlrx1*^{-/-} mice, relative to the responses in their wild-type counterparts (Fig. 1h).

Supplementing PH5CH8 cells with the antioxidant NAC (N-acetyl-L-cysteine) did not abolish the positive effect of NLRX1 deficiency on the replication of an HCV reporter virus, nor did treating cells with an inhibitor of endoplasmic reticulum stress (TUDCA) or autophagy (3-MA) (Supplementary Fig. 1b). Thus, the increased HCV replication in NLRX1-deficient cells was probably not due to diminished production of reactive oxygen species^{11,17} or to the influence of NLRX1 depletion on autophagy or the response to endoplasmic reticulum stress^{18,19}.

To ascertain whether the proviral effect of NLRX1 deficiency resulted from a reduction in early innate immune response, we designed a Transwell assay for soluble antiviral factors (Supplementary Fig. 1c). We assessed replication of an HCV reporter virus in indicator cells separated by a permeable membrane from NLRX1-deficient cells or control PH5CH8 cells, each stimulated by replication-competent HCV RNA, and found greater replication of the reporter virus in indicator cells exposed to NLRX1-deficient cells than in those exposed to control PH5CH8 cells (Supplementary Fig. 1c). Inhibition of JAK-STAT signaling with ruxolitinib (an inhibitor of JAK1 and JAK2) or tofacitinib (an inhibitor of JAK3) also substantially reduced the difference in HCV replication in NLRX1-T3 cells relative to that in control PH5CH8 cells (Supplementary Fig. 1d), consistent with the suppression of viral replication by cytokine responses involving JAK signaling. Depleting cells of NLRX1 had no effect on the replication of HAV or HCV in RIG-I-deficient Huh-7.5 human hepatoma cells²⁰ (Supplementary Fig. 1e) or in MAVS-deficient PH5CH8 cells (Supplementary Fig. 1f). Collectively, these results defined NLRX1 as a positive regulator of soluble RIG-I- and MAVS-mediated antiviral responses in human hepatocytes.

NLRX1 regulates IRF3 and IRF1 responses differentially

We carried out a series of dual-luciferase-promoter assays to determine if NLRX1 directly regulated the transcription of cytokine-encoding genes. NLRX1 deficiency had little effect on the basal activity of the NF- κ B-responsive promoter PRDII but modestly reduced its activation by SeV (Fig. 2a). Consistent with that, overexpression of NLRX1 enhanced the activation of PRDII triggered by SeV (Fig. 2a). In contrast, NLRX1 deficiency minimally affected activation of the *IFNB1* promoter and had no effect on the IRF3-responsive promoter 4*PRD(I/III) (Supplementary Fig. 2a,b). We also assessed the effect of NLRX1 deficiency on the stability of *IL6* mRNA, as IL-6 expression is regulated in part through 3' untranslated region (UTR) sequences programmed for rapid mRNA turnover²¹. NLRX1 deficiency had no effect on *IL6* mRNA decay in cells treated with actinomycin D (Supplementary Fig. 2c), nor did overexpression of NLRX1 alter luciferase expression from mRNA transcripts containing the *IL6* 3' UTR (Supplementary Fig. 2d). In aggregate, these data suggested that NLRX1 had a positive but limited effect on the activation of NF- κ B-responsive promoters by SeV and had no influence on the stability of *IL6* mRNA.

To more directly investigate the influence of NLRX1 deficiency on the activation of NF- κ B, we assessed SeV-induced signaling via the NF- κ B subunit RELA (p65). NLRX1 deficiency minimally affected phosphorylation of the inhibitory cytoplasmic NF- κ B chaperone NFKBIA (I κ B α) or RELA in SeV-infected PH5CH8 cells (Supplementary Fig. 2e). An electrophoretic mobility-shift assay with an NF- κ B probe revealed a significant but quantitatively small decrease in the intensity of SeV-induced band shifts in NLRX1-deficient (NLRX1-T2 and NLRX1-T3) PH5CH8 cells relative to that

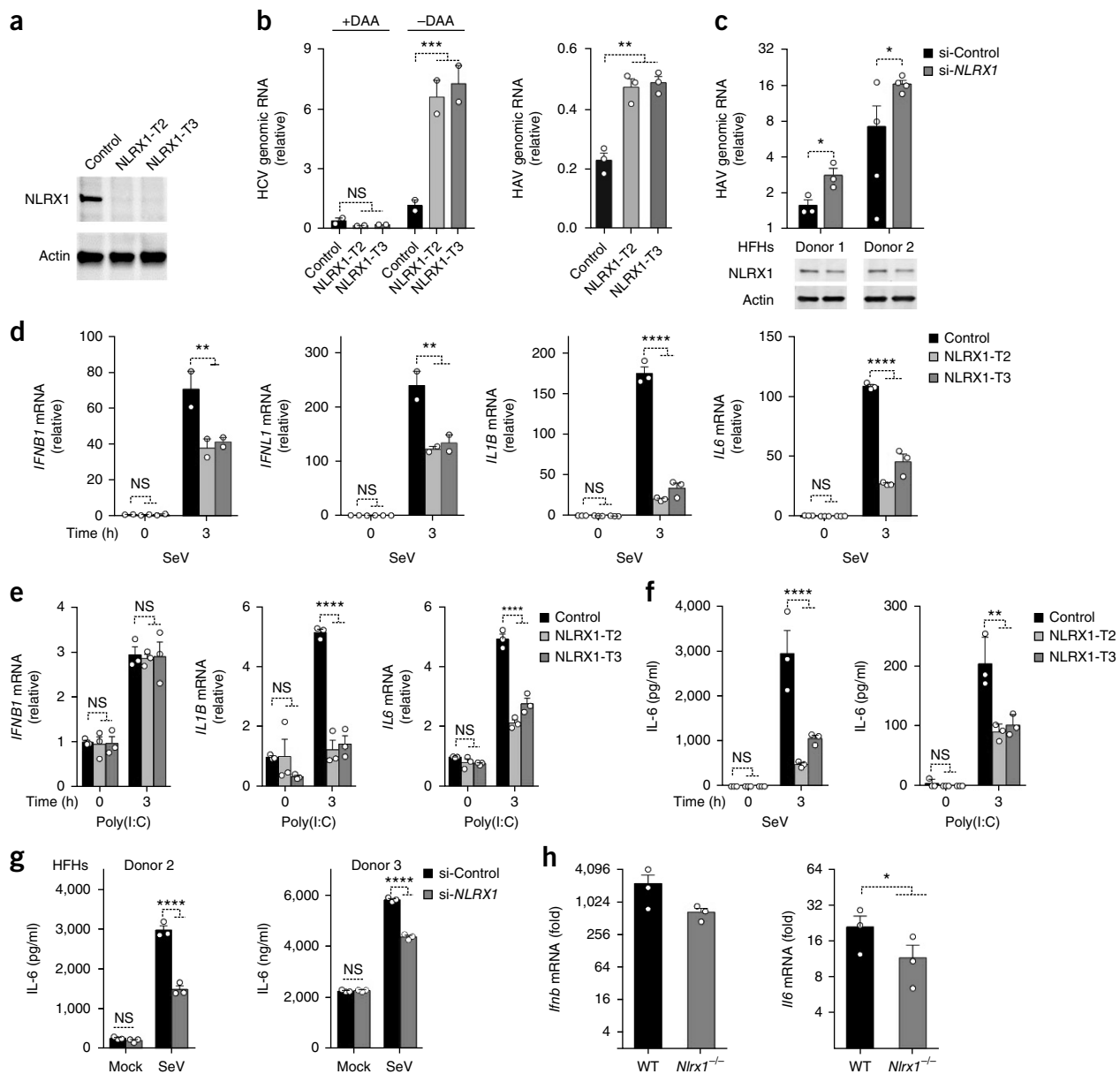


Figure 1 NLRX1 is a positive regulator of innate immunity and an antiviral factor in hepatocytes. **(a)** Immunoblot analysis of NLRX1 and actin (loading control throughout) in control PH5CH8 cells (Control), NLRX1-T2 cells and NLRX1-T3 cells (above lanes). **(b)** qRT-PCR analysis of genomic RNA from HCV (left) and HAV (right) in control PH5CH8 cells, NLRX1-T2 cells and NLRX1-T3 cells (horizontal axis) transfected for 24 h with HCV RNA, in the presence (+DAA) or absence (-DAA) of a direct-acting antiviral inhibitor (left) or infected for 72 h with HAV (right); result are presented relative to the abundance of viral RNA at 6 h (left) or in control PH5CH8 cells at 24 h (right). **(c)** qRT-PCR analysis (top) of HAV genomic RNA in primary HFHs (from two different donors; horizontal axis) at 72 h after treatment with control siRNA (si-Control) or partial depletion of NLRX1 with *NLRX1*-specific siRNA (si-*NLRX1*) (key), presented relative to the abundance of viral RNA at 5 h; below, immunoblot analysis of NLRX1 in the cells above. **(d,e)** qRT-PCR analysis of *IFNB1*, *IFNL1*, *IL1B* and *IL6* mRNA in control PH5CH8 cells, NLRX1-T2 cells and NLRX1-T3 cells (key) left uninfected (0) or infected for 3 h with SeV (d) or left untreated (0) or stimulated with poly(I:C) added to medium for 3 h (e); results were normalized to those of *ACTB*. **(f,g)** ELISA of IL-6 in control PH5CH8 cells, NLRX1-T2 cells and NLRX1-T3 cells (key) infected with SeV as in **d** or stimulated with poly(I:C) as in **e** (horizontal axis) (f), and in HFHs treated with siRNA as in **c** (key) and mock infected or infected with SeV (horizontal axis) (g). **(h)** qRT-PCR analysis of *Ifnb* and *Il6* mRNA in the liver of wild-type (WT) and *Nlr1*^{-/-} mice (horizontal axis) 3 h after hydrodynamic injection of HAV RNA; results were normalized to those of *Actb*. Each symbol (**b-h**) represents an individual technical replicate (**b-d** (*IL1B* and *IL6*), **e-g**), experiment (**d**, *IFNB1* and *IFNL1*) or mouse (**h**) (mean + s.e.m in each). NS, not significant ($P > 0.05$); * $P < 0.05$, ** $P < 0.01$, *** $P < 0.001$ and **** $P < 0.0001$, control cells versus cells depleted of NLRX1 (except where indicated otherwise) (two-way analysis of variance (ANOVA) (b (left), **d-f**) or *t* test (b (right), **c,g,h**)). Data are representative of three experiments (**a**), three independent experiments with $n = 2$ (left) or $n = 3$ (right) technical replicates (**b**), two experiments with $n = 3$ (donor 1) or $n = 4$ (donor 2) technical replicates (**c**), three experiments with $n = 3$ technical replicates in each (**d** (*IL1B* and *IL6*), **e**), three experiments (**f**) or two experiments with two donors (**g**), with $n = 3$ technical replicates in each (**f,g**) or one experiment with $n = 3$ mice per genotype (**h**) or are from two independent experiments with $n = 4$ technical replicates (**d**, *IFNB1* and *IFNL1*).

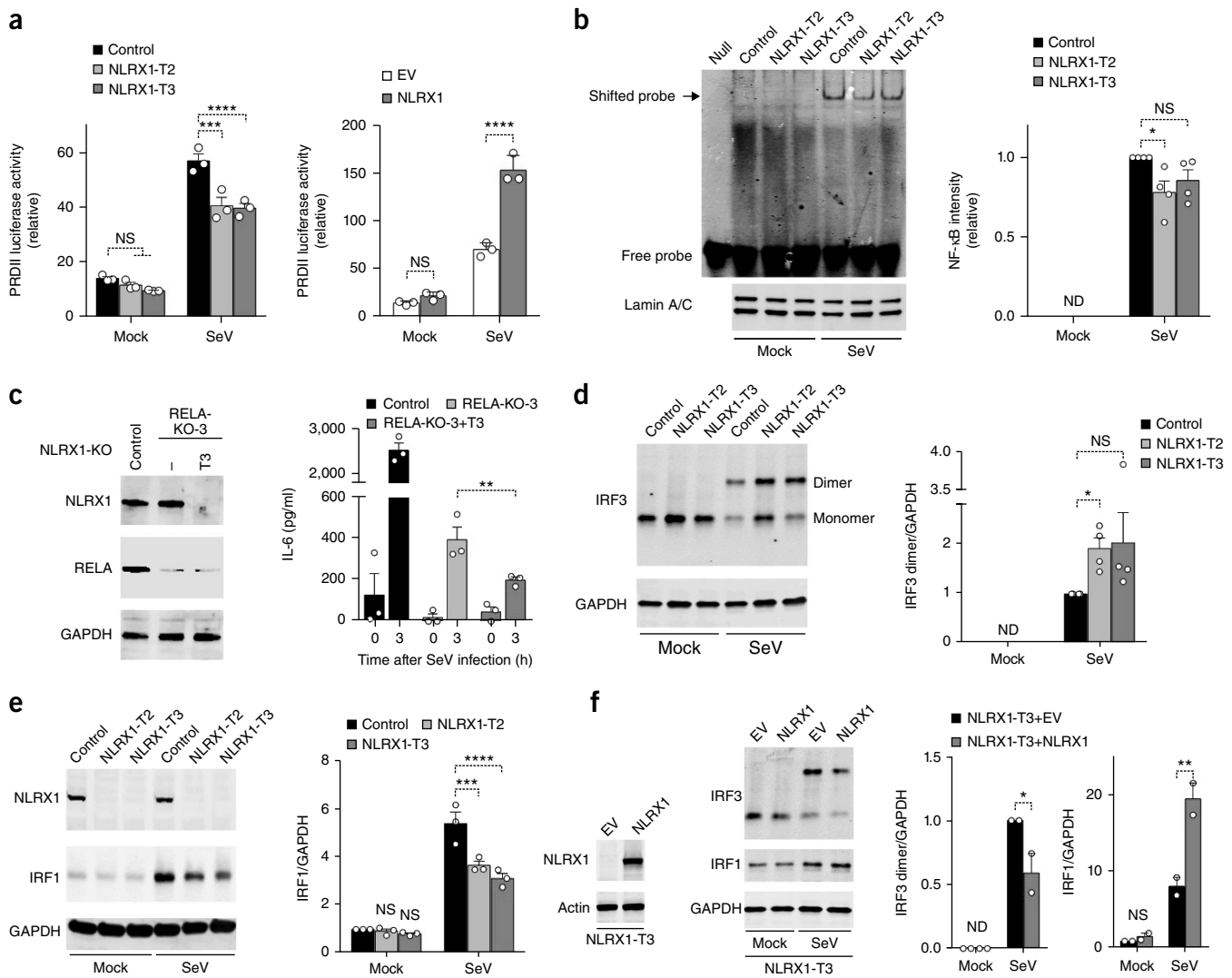


Figure 2 Effect of NLRX1 deficiency on NF- κ B signaling and the activation of IRF1 and IRF3 in SeV-infected PH5CH8 cells. **(a)** Activity of a (firefly) luciferase reporter for the promoter PRDII in control PH5CH8 cells, NLRX1-T2 cells and NLRX1-T3 cells (key) (left) or PH5CH8 cells transfected with empty vector (EV) or transfected to overexpress NLRX1 (key) (right), all mock infected or infected with SeV (horizontal axis); results are presented relative to renilla luciferase activity. **(b)** Electrophoretic mobility-shift assay of NF- κ B without nuclear extracts (Null) or with nuclear extracts from control PH5CH8 cells, NLRX1-T2 cells and NLRX1-T3 cells (above lanes) mock infected or infected with SeV (below blot) (top left), together with immunoblot analysis of lamin A/C as a loading control (bottom left) and mean infrared fluorescence intensity of the shifted probe (assessed as at left), presented relative to that in SeV-infected control PH5CH8 cells (right). ND, not detected. **(c)** Immunoblot analysis of NLRX1, RELA and GAPDH (loading control throughout) in NLRX1- and RELA-sufficient PH5CH8 cells (Control), RELA-deficient PH5CH8 cells (RELA-KO-3, NLRX1-KO -) and PH5CH8 cells doubly deficient in NLRX1 and RELA (RELA-KO-3, NLRX1-KO T3) (above lanes) (left), and ELISA of IL-6 in cells as at left (key), left uninfected (0) or infected for 3 h with SeV (horizontal axis) (right). **(d,e)** Immunoblot analysis (left) of IRF3 monomers and dimers (right margin) **(d)** and of NLRX1 and IRF1 (left margin) **(e)** in control PH5CH8 cells, NLRX1-T2 cells and NLRX1-T3 cells (above lanes) mock infected or infected with SeV (below blots); right, quantification of the intensity of IRF3 dimers **(d)** or IRF1 **(e)**, relative to that of GAPDH. **(f)** Immunoblot analysis of NLRX1 (far left) or IRF3 and IRF1 (middle left) in NLRX1-T3 cells transfected with empty lentivirus vector (EV) or with lentivirus vector encoding NLRX1 (above lanes) and left uninfected (far left) or mock infected or infected with SeV (below blots) (middle left); right, quantification of the intensity of IRF3 dimers (middle right) or IRF1 (far right), relative to that of GAPDH. Each symbol represents an individual technical replicate **(a,c)** or experiment **(b,d-f)** (mean + s.e.m. throughout). * $P < 0.05$, ** $P < 0.01$, *** $P < 0.001$ and **** $P < 0.0001$, control cells versus cells depleted of NLRX1 (two-way ANOVA **(a,e)** and t test **(b-d,f)**). Data are representative of three independent experiments with $n = 3$ technical replicates **(a)**, four **(b,d)**, three **(e)** or two **(f)** independent experiments **(b,d-f)**, or two independent experiments with $n = 3$ technical replicates in each **(c)**.

in control PH5CH8 cells (**Fig. 2b**). We concluded from these data that NLRX1 deficiency minimally suppressed SeV-induced NF- κ B signaling in PH5CH8 cells and that this subtle impairment of NF- κ B signaling probably did not explain the marked reductions we observed in cytokine expression.

To further test our hypothesis, we assessed how depleting RELA influenced IL-6 production after SeV infection and the modulation of IL-6 expression by NLRX1 in PH5CH8 cells. As anticipated, RELA deficiency caused a large decrease in the SeV-induced expression of IL-6 protein (**Fig. 2c**). Notably, however, eliminating NLRX1

expression resulted in a further reduction in IL-6 production in RELA-deficient cells (Fig. 2c). Thus, the negative effect of NLRX1 deficiency on the IL-6 response that we observed in RELA-replete cells was preserved in RELA-deficient cells. Collectively, these results

indicated that NLRX1 regulated IL-6 production downstream and independently of NF- κ B.

Although our data showed that IL-6 was strongly regulated by NF- κ B in PH5CH8 cells (Fig. 2c), CRISPR-Cas9-mediated depletion of

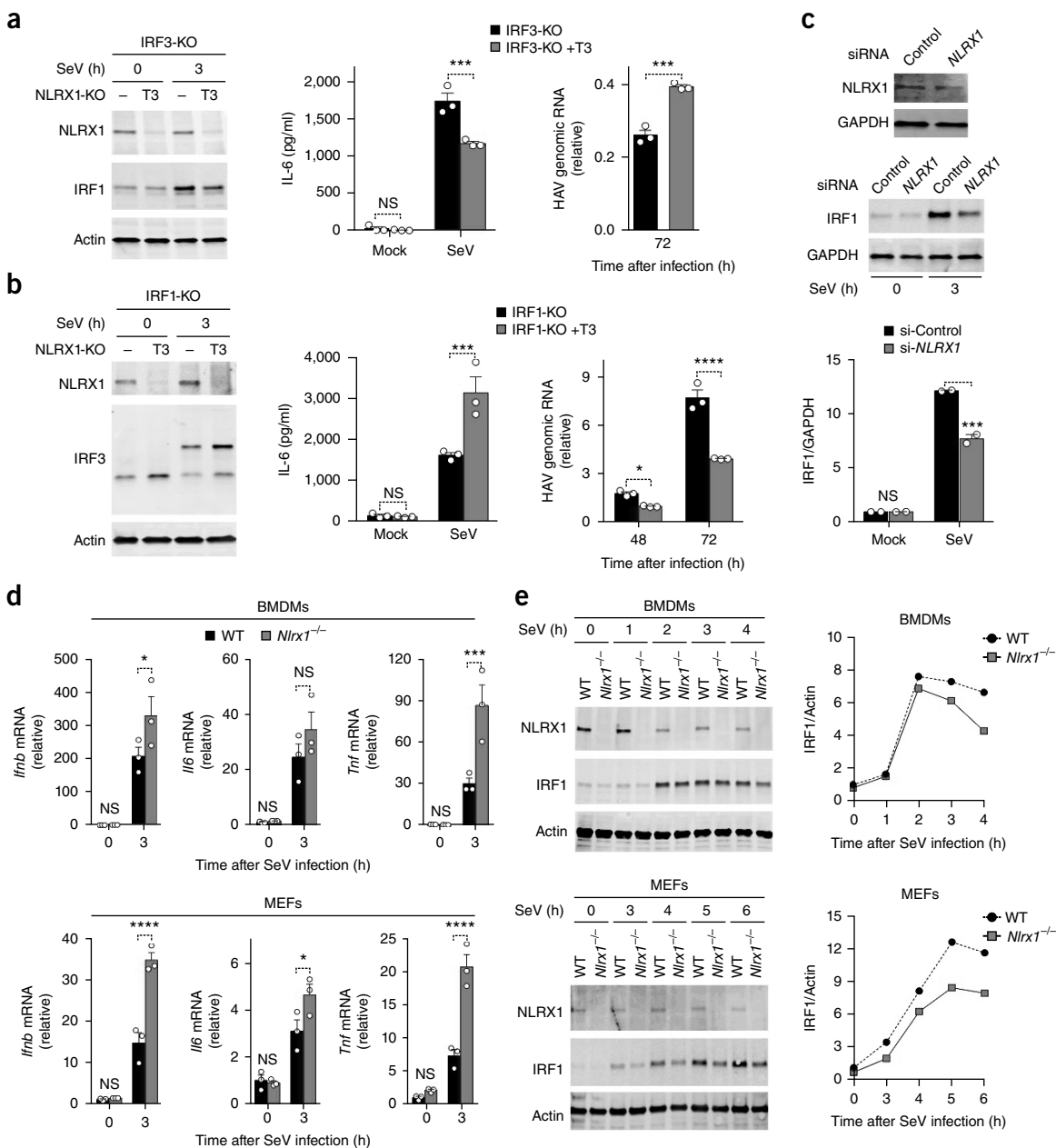


Figure 3 NLRX1-IRF1 signaling dominates the antiviral cytokine response in hepatocytes. (a,b) ELISA of IL-6 (middle) and qRT-PCR analysis of HAV genomic RNA (right) in IRF3-deficient PH5CH8 cells (IRF3-KO) and PH5CH8 cells doubly deficient in IRF3 and NLRX1 (IRF3-KO + T3) (a), or in IRF1-deficient PH5CH8 cells (IRF1-KO) and PH5CH8 cells doubly deficient in IRF1 and NLRX1 (IRF1-KO + T3) (b), mock infected or infected for 3 h with SeV (a,b, middle) or for 72 h with HAV (a, right) or infected for 48 or 72 h with HAV (b, right) (horizontal axes) and immunoblot analysis (left) of NLRX1 and IRF1 (a) or of NLRX1 and IRF3 dimers (b) in cells as at right, left uninfected (0) or infected for 3 h with SeV (above lanes) (immunoblot analysis of IRF1-deficient and IRF3-deficient cells, **Supplementary Fig. 2f**); qRT-PCR results are presented relative to those of cells at 4 h. (c) Immunoblot analysis of NLRX1 and IRF1 in FHFs treated with control siRNA or partially depleted of NLRX1 via *NLRX1*-specific siRNA (above lanes) (top) or treated with siRNA as above and left uninfected (0) or infected for 3 h with SeV (below blot) (middle), and quantification of IRF1 (infrared fluorescence intensity) in immunoblot analysis as above, relative to that of GAPDH. (d,e) qRT-PCR analysis of *Ifnb*, *Il6* and *Tnf* mRNA (d), immunoblot analysis of NLRX1 and IRF1 (e, left) and quantification of IRF1 as in c (e, right) in wild-type and *Nlr1^{-/-}* BMDMs (top) or MEFs (bottom) left uninfected (0) or infected for 3 h (d) or 1-6 h (e) with SeV. Each symbol (a-d) represents an individual technical replicate (a,b,d) or donor (c) (mean + s.e.m in each). * $P < 0.05$, ** $P < 0.01$, *** $P < 0.001$ and **** $P < 0.0001$ (t -test). Data are representative of two to three independent experiments with $n = 3$ technical replicates in each (a,b), two experiments with two donors (c) or four (BMDM) or two (MEF) independent experiments with $n = 3$ technical replicates in each (d), or are representative of two independent experiments (e).

either of two members of the IRF family of transcription factors, IRF1 and IRF3, suppressed early (3-hour) *IL1B* and *IL6* mRNA and IL-6 protein responses to SeV (**Supplementary Fig. 2f–h**). Because IRF1 and IRF3 regulate the induction of *IFNB1* and *IFNL1* transcripts in human hepatoma cells²², we assessed the effect of NLRX1 deficiency on IRF3 and IRF1 responses in PH5CH8 cells. IRF3 is constitutively expressed and is activated by phosphorylation, which leads to its dimerization and cytoplasmic–nuclear translocation²³. NLRX1 deficiency significantly enhanced this response and led to an increase in the SeV-induced formation of IRF3 dimers (**Fig. 2d**). Basal expression of IRF1 protein was low in mock-infected cells but was substantially induced by infection with SeV (**Fig. 2e**). In contrast to the enhancement observed in the activation of IRF3, NLRX1 deficiency significantly reduced the SeV-triggered increases in the abundance of IRF1 (**Fig. 2e**). Reconstituting NLRX1 expression in NLRX1-T3 cells with recombinant lentivirus reversed both of those changes (**Fig. 2f**). Collectively, these data revealed that NLRX1 regulated SeV-induced IRF3 signaling and IRF1 signaling in hepatocytes differentially, suppressing the activation of IRF3 but enhancing increases in IRF1 expression.

NLRX1's promotion of IRF1 dominates in hepatocytes

Because NLRX1 deficiency suppresses innate immunological control of viral replication in hepatocytes, we reasoned that the positive regulation of IRF1 by NLRX1, rather than its negative regulation of IRF3, probably dominates cytokine responses in hepatocytes. To test our hypothesis, we depleted IRF1- and IRF3-deficient PH5CH8 cells of NLRX1 expression and assessed responses to SeV challenge in the resulting NLRX1–IRF3 or NLRX1–IRF1 doubly deficient cells. In IRF3-deficient cells, the IRF1 and IL-6 protein responses to infection with SeV were suppressed and HAV replication was enhanced by depletion of NLRX1 (**Fig. 3a**). Thus, the effect of NLRX1 depletion in IRF3-deficient PH5CH8 cells was similar to that in unmodified PH5CH8 cells. In contrast, depleting IRF1-deficient cells of NLRX1 enhanced the formation of IRF3 dimers (as in IRF1-replete cells) but enhanced the SeV-induced production of IL-6 and also suppressed HAV replication (**Fig. 3b**). Thus, the effects of NLRX1 depletion on cytokine expression and viral replication were reversed in IRF1-deficient cells, which suggested that the NLRX1–IRF1 signaling axis is dominant in hepatocytes. Consistent with that conclusion, the reduced production of IL-6 in SeV-infected HFHs depleted of NLRX1 (**Fig. 1g**) was accompanied by a reduction in the accumulation of IRF1 protein (**Fig. 3c**).

Most reports suggest that rather than enhancing such responses, NLRX1 suppresses, early innate immune responses in bone-marrow-derived macrophages (BMDMs) and primary MEFs^{6–8}. Thus, we sought to determine whether IRF1 signaling was negatively or positively regulated by NLRX1 in these cell types. Consistent with a suppressive effect on innate immunity, we found that loss of NLRX1 enhanced the SeV-mediated *Ifnb*, *Tnf* and *Il6* mRNA responses in mouse BMDMs and MEFs (**Fig. 3d**). Despite that, NLRX1 deficiency reduced the SeV-triggered increase in the abundance of IRF1 protein in both cell types (**Fig. 3e**). Thus, the positive regulation of IRF1 signaling by NLRX1 was not specific to hepatocytes or human cells. The finding that cytokine responses were enhanced, while IRF1 induction was decreased, in BMDMs and MEFs depleted of NLRX1 indicated that IRF1 did not have a dominant role in determining cytokine responses in these cells. Thus, the ultimate effect of NLRX1 on early antiviral responses was determined by whether IRF1 or IRF3 dominated in driving the response.

NLRX1 enhances IRF1 protein synthesis in infected cells

IRF1 is the ‘founding member’ of the IRF family, and its expression is induced rapidly by viral infection^{24,25}. However, the mechanisms that mediate this response are poorly understood. Given its role in initiating IRF3-directed responses to SeV in hepatocytes²⁰, we reasoned that RIG-I and its adaptor MAVS might mediate the IRF1 response. Consistent with that, depleting cells of MAVS significantly suppressed both IRF3 responses and IRF1 responses to SeV infection in PH5CH8 cells (**Supplementary Fig. 3a**). The loss of SeV-induced dimerization of IRF3 and expression of IRF1 protein was not reversed by additional depletion of NLRX1 in MAVS-deficient PH5CH8 cells (**Supplementary Fig. 3a**).

Consistent with published studies showing that increased *IRF1* transcription drives the IRF1 protein response to viral infection²⁵, globally inhibiting transcription with actinomycin D completely abolished the IRF1 protein response to SeV (**Supplementary Fig. 3b**). To better understand how NLRX1 might regulate this IRF1 response, we assessed the roles of IRF3 and NF- κ B. Notably, depleting cells of IRF3 had no effect on either the transcription of *IRF1* or the expression of IRF1 protein (**Supplementary Fig. 3c**). In contrast, depleting cells of RELA significantly suppressed both the transcription of *IRF1* and the increase in expression of IRF1 protein in response to SeV in PH5CH8 cells (**Supplementary Fig. 3d**). siRNA-mediated silencing of *NFKB1*, which encodes the NF- κ B subunit p50, modestly diminished the IRF1 protein response to SeV infection, and in combination with RELA deficiency, it substantially reduced the SeV-induced abundance of *IRF1* transcripts (**Supplementary Fig. 3e,f**). Collectively, these data demonstrated that the immediate (3-hour) increase in the expression of IRF1 protein in response to infection with SeV was driven by signaling via MAVS and NF- κ B in PH5CH8 cells.

Notably, although NLRX1 deficiency modestly enhanced the SeV-induced abundance of *IRF3* transcripts (**Supplementary Fig. 4a**), it had no effect on either the abundance of *IRF1* transcripts (**Fig. 4a**) or the stability of *IRF1* mRNA (**Fig. 4b**). These data were in agreement with our earlier observations indicating an only modest impairment of NF- κ B signaling in NLRX1-deficient cells (**Fig. 2b**) and collectively indicated that NLRX1 regulated IRF1 expression post-transcriptionally. To gain insight into whether this negative regulation of the IRF1 response was due to enhanced degradation of IRF1 or reduced synthesis of IRF1 protein, we globally inhibited protein synthesis in SeV-infected cells with cycloheximide and monitored the subsequent decay of IRF1 protein. Despite the greater initial abundance of IRF1 in control PH5CH8 cells than in NLRX1-T3 cells, the half-life (stability) of IRF1 protein in NLRX1-T3 cells was indistinguishable from that in control PH5CH8 cells (**Fig. 4c** and **Supplementary Fig. 4b**). Collectively, these data suggested that the reduced abundance of IRF1 protein in NLRX1-deficient cells resulted from impaired translation of *IRF1* mRNA. Consistent with that, globally blocking protein synthesis with puromycin completely abolished the effect of NLRX1 deficiency on the IRF1 response to infection with SeV (**Supplementary Fig. 4c**).

To determine how NLRX1 might influence protein synthesis, we measured the incorporation of [³⁵S]-labeled methionine and cysteine ([³⁵S]-Met-Cys) into protein. Protein synthesis in NLRX1-T3 cells was qualitatively similar to that in control PH5CH8 cells, both before infection with SeV and after such infection (**Supplementary Fig. 4d**). However, whereas infection with SeV induced a significant, quantitative increase in protein synthesis in control PH5CH8 cells, it had a much smaller, nonsignificant effect on NLRX1-T3 cells (**Fig. 4d**). The absence of any novel protein bands incorporating [³⁵S]-Met-Cys that were not

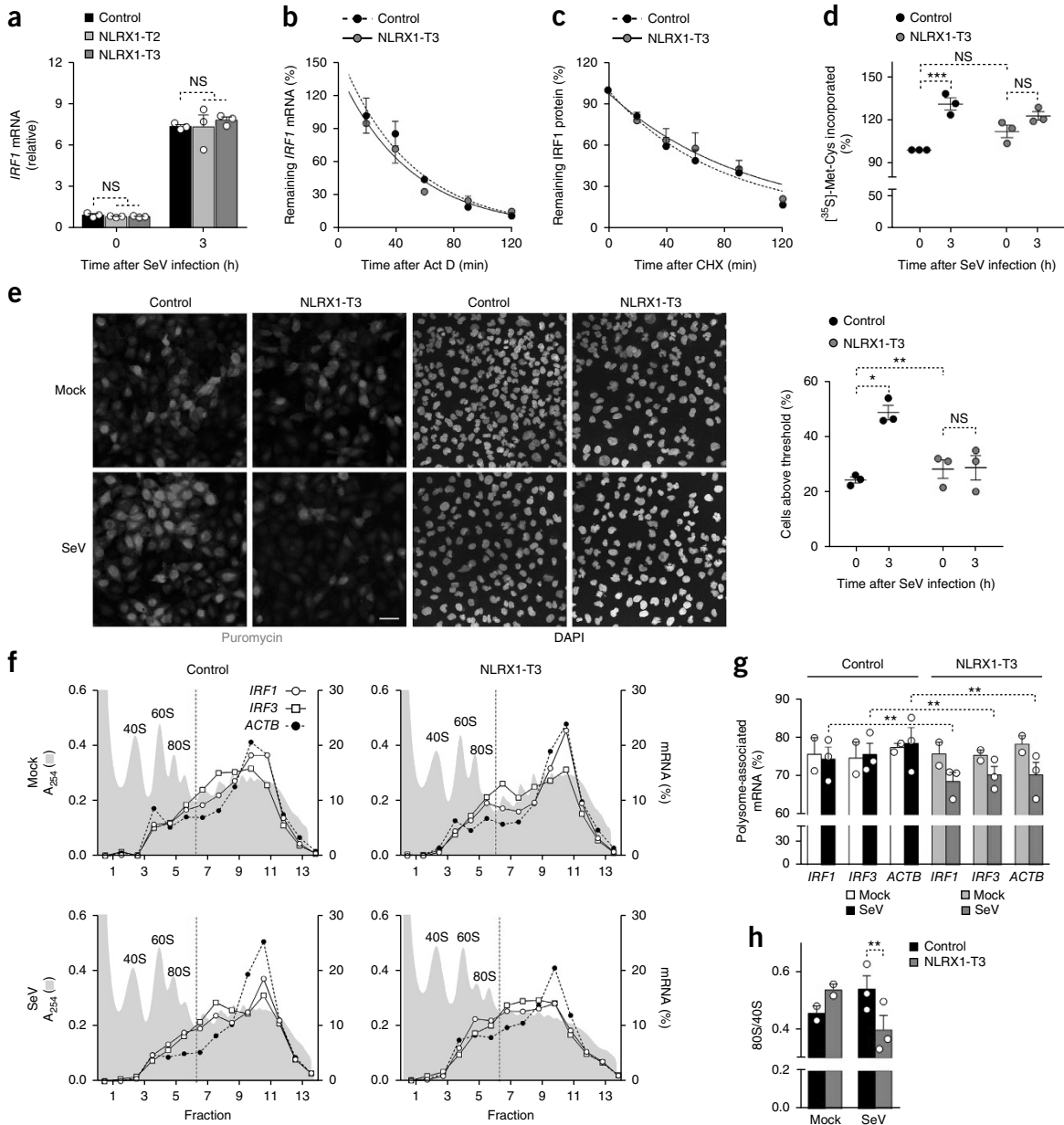


Figure 4 NLRX1 facilitates immediate IRF1 antiviral responses by promoting global protein synthesis in SeV-infected cells. **(a)** qRT-PCR analysis of *IRF1* mRNA in control PH5CH8 cells, NLRX1-T2 cells and NLRX1-T3 cells (key) left uninfected (0) or infected for 3 h with SeV (horizontal axis); results were normalized to those of *ACTB*. **(b)** Stability of *IRF1* mRNA in SeV-infected control PH5CH8 cells and NLRX1-T3 cells (key), assessed as *IRF1* mRNA remaining at various times (horizontal axis) after treatment with actinomycin D (Act D). **(c)** Stability of IRF1 protein in SeV-infected control PH5CH8 cells and NLRX1-T3 cells (key), assessed by quantification of band intensity (immunoblot analysis, **Supplementary Fig. 4b**) at various times (horizontal axis) after treatment with cycloheximide (CHX). **(d)** Nascent protein synthesis in control PH5CH8 cells and NLRX1-T3 cells (key) mock infected (0) or infected for 3 h with SeV, assessed as the incorporation of [³⁵S]-Met-Cys into cellular proteins (precipitated from cells by trichloroacetic acid), relative to that in uninfected control PH5CH8 cells, set as 100% (immunoblot analysis, **Supplementary Fig. 4d**). **(e)** Confocal microscopy (left) of control PH5CH8 cells and NLRX1-T3 cells mock infected (0) or infected for 3 h with SeV (left margin) and pulse-labeled with puromycin, assessing global protein synthesis by staining of puromycin with specific antibody, with nuclei counterstained with the DNA-binding dye DAPI (below images), and frequency of cells with puromycin labeling exceeding an arbitrary threshold (far right). Scale bar (left), 40 μ m. **(f)** Polysome profile of *IRF1*, *IRF3* or *ACTB* mRNA in mock- or SeV-infected (left margin) control PH5CH8 cells and NLRX1-T3 cells (key), plotted as absorbance at 254 nm (A_{254}) (left vertical axis) and qRT-PCR analysis of mRNA (presented as percent of total mRNA in each fraction; right vertical axis); red vertical lines distinguish polysome-associated mRNA (fractions 7–14) from non-polysome-associated mRNA (fractions 1–6). **(g)** Proportion of *IRF1*, *IRF3* or *ACTB* mRNA (horizontal axis) associated with translationally active polysomes (fractions 7–14 in **f**) in control PH5CH8 cells and NLRX1-T3 cells (above plot) mock infected or infected with SeV (key). **(h)** Ratio of 80S to 40S in mock- or SeV infected (horizontal axis) control PH5CH8 cells and NLRX1-T3 cells (key), calculated from the area under the curve of 40S and 80S peaks of A_{254} traces. Each symbol (**a,d,e,g,h**) represents an individual technical replicate (**a**) or experiment (**d,e,g,h**); small horizontal lines (**d,e**) indicate the mean (\pm s.e.m.). * $P < 0.05$, ** $P < 0.01$ and *** $P < 0.001$ (two-way ANOVA (**a,d,e,g**) or *t*-test (**h**)). Data are representative of three experiments with $n = 3$ technical replicates in each (**a**; mean \pm s.e.m.), two experiments with $n = 3$ technical replicates (**b**; mean \pm s.e.m.), six experiments (**c**; mean \pm s.e.m.), three experiments with $n = 1-3$ technical replicates (**d**), three experiments (**e**, left), three experiments with an average of 176 cells per condition (**e**, right), or two to three experiments (**f-h**; mean \pm s.e.m. in **g,h**).

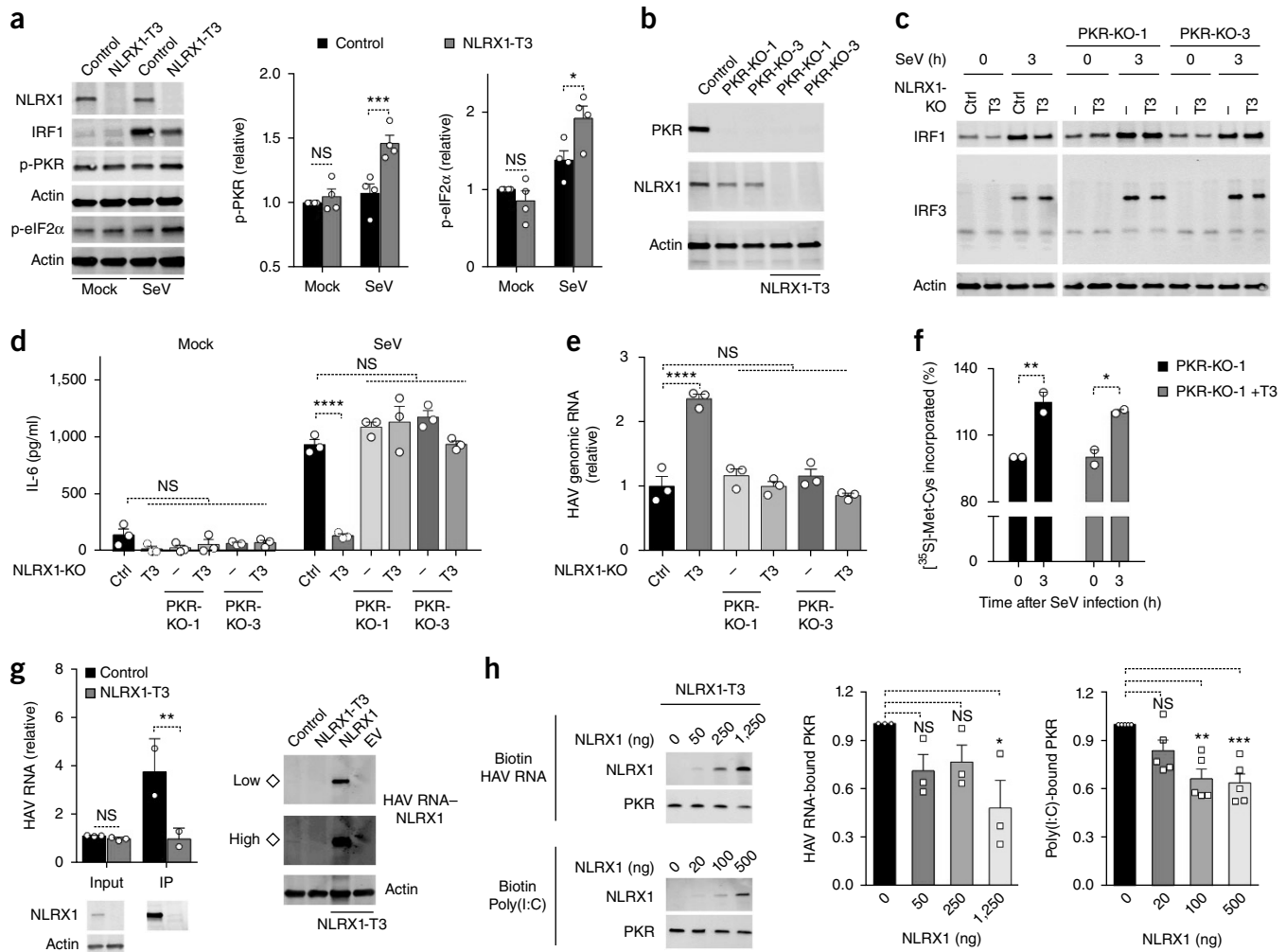


Figure 5 NLRX1 reduces the activation of PKR and subsequent inhibition of protein synthesis by competing for binding to viral RNA. (a) Immunoblot analysis of total NLRX1 and IRF1 and phosphorylated (p-) PKR and eIF2 α (left margin) in control PH5CH8 cells and NLRX1-T3 cells (above lanes) mock infected or at 4.5 h after infection with SeV (below blots), assessing PKR-eIF2 α signaling (left), and quantification (infrared fluorescence intensity) of phosphorylated PKR or eIF2 α , normalized to that of actin (right). (b) Immunoblot analysis of PKR and NLRX1 in control PH5CH8 cells (left) or PKR-deficient PH5CH8 cells (PKR-KO-1 or PKR-KO-3 (above lanes); middle) or PH5CH8 cells deficient in both NLRX1 and PKR (PKR-KO-1 or PKR-KO-3 (above lanes) plus NLRX1-T3 (below blot); right). (c) Immunoblot analysis of IRF1 (top) and IRF3 dimers (middle) in control PH5CH8 cells (Ctrl) and NLRX1-T3 cells (T3) (left blots) or PKR-deficient PH5CH8 cells (PKR-KO-1 or PKR-KO-3 (above blots) and - (above lanes); right) or PH5CH8 cells deficient in both NLRX1 and PKR (PKR-KO-1 or PKR-KO-3 (above blots) and T3 (above lanes); right). (d,e) ELISA of IL-6 (d) and qRT-PCR analysis of HAV RNA (e) in cells as in c (below plots); qRT-PCR results are presented relative to those of control PH5CH8 cells, set as 1. (f) Global protein synthesis in PKR-deficient PH5CH8 cells (PKR-KO-1) and PH5CH8 cells deficient in both NLRX1 and PKR (PKR-KO-1 + T3) (key) mock infected (0) or infected for 3 h with SeV (horizontal axis), assessed as incorporation of [³⁵S]-Met-Cys (as in Fig. 4d). (g) qRT-PCR analysis of HAV RNA (top left) and immunoblot analysis of NLRX1 (bottom left) in control PH5CH8 cells and NLRX1-T3 cells (key) transfected for 3 h with HAV RNA, assessed as input samples or after immunoprecipitation (IP) with antibody to NLRX1 (horizontal axis or above lanes). Right, immunoblot analysis of NLRX1 precipitated together with biotin-tagged HAV RNA (HAV RNA-NLRX1; right margin) in lysates of control PH5CH8 cells or NLRX1-T3 cells (left half) or NLRX1-T3 cells (below blot) transfected with empty vector or vector expressing NLRX1 (above lanes; right half); left margin (\diamond), endogenous NLRX1 associated with HAV RNA, with high or low detection intensity. (h) Immunoblot analysis (left) of NLRX1 and PKR in lysates of NLRX1-T3 cells supplemented with various doses (above lanes) of purified recombinant NLRX1 and with biotin-tagged HAV RNA (top) or poly(I:C) (bottom); right, quantification of the binding of HAV RNA (near right) or poly(I:C) (far right) to PKR. Each symbol (a,d,e,f,g,h) represents an individual experiment (a,f,g,h) or technical replicate (d,e) (mean + s.e.m in each). * $P < 0.05$, ** $P < 0.01$ and *** $P < 0.001$ (two-way ANOVA (a,d,f,g) or one-way ANOVA (e,h)). Data are representative of four independent experiments (a), two independent experiments (b,c), two experiments with $n = 3$ technical replicates in each (d,e), two experiments with $n = 2$ technical replicates (f), two experiments with $n = 2-3$ technical replicates (g) or three (HAV RNA) or five (poly(I:C)) experiments (h).

present in the lysates of uninfected cells (Supplementary Fig. 4d) indicated that this increase was due to enhanced cellular protein synthesis, not viral protein synthesis. As an independent measure of protein synthesis, we pulse-labeled NLRX1-T3 cells with a low concentration of puromycin and used confocal microscopy to monitor its incorporation into nascent protein at a single-cell level

(Fig. 4e). Infection with SeV induced an increase in nascent protein synthesis in a large proportion of control PH5CH8 cells but not in NLRX1-T3 cells (Fig. 4e). We obtained similar results with NLRX1-T2 cells, at both a whole-cell-culture level and a single-cell level of analysis (Supplementary Fig. 4e), which excluded the possibility that this reflected an off-target effect of the sgRNA used to create the

NLRX1-T3 cells. siRNA-mediated depletion of NLRX1 expression in primary HFHs also substantially suppressed the SeV-induced increases in nascent protein synthesis (**Supplementary Fig. 4f**).

Although NLRX1 exerted distinctly different regulatory effects on SeV-induced cytokine expression in MEFs relative to that human hepatocytes, depleting cells of NLRX1 expression reduced the SeV-induced increase in the abundance of IRF1 in both cell types (**Figs. 2e** and **3e**). Consistent with that finding, the incorporation of puromycin into nascent protein was also significantly lower in SeV-infected MEFs from *NlrX1*^{-/-} mice than in those from wild-type mice (**Supplementary Fig. 4g**). Thus, the negative effect of NLRX1 deficiency on protein synthesis in virus-infected cells was not limited to human hepatocytes.

To directly characterize the effect of NLRX1 deficiency on the translation of mRNA by ribosomes, we used sucrose-density-gradient fractionation to profile polysome formation following the infection of NLRX1-T3 cells or control PH5CH8 cells with SeV (**Fig. 4f**). The deletion of NLRX1 resulted in a significant shift in the gradient distribution of *IRF1*, *IRF3* and *ACTB* mRNA from SeV-infected cells, with a significantly lower proportion of each mRNA associated with translationally active polysomes (fractions 7–13) (**Fig. 4g**). Moreover, the formation of translationally competent 80S ribosomes was lower in SeV-infected NLRX1-T3 cells than in SeV-infected control PH5CH8 cells, as shown by the much lower ratio of 80S to the 40S subunit in SeV-infected NLRX1-T3 cells than in SeV-infected control PH5CH8 cells (**Fig. 4h** and **Supplementary Fig. 4h**); this suggested a defect in initiation of translation. Collectively, these three separate measures of protein synthesis—incorporation of [³⁵S]-Met-Cys, puromycin labeling and polysome profiling—indicated that the translation of mRNA was globally suppressed by the absence of NLRX1 expression in SeV-infected cells.

NLRX1 limits PKR-mediated global translational shutdown

The dsRNA-activated kinase PKR is triggered by viral infection to phosphorylate the translation-initiation factor eIF2 α and thereby globally shuts down host-cell translation²⁶. To ascertain whether NLRX1 influences that PKR response, we characterized the activation of PKR in NLRX1-deficient cells. NLRX1 deficiency enhanced the SeV-induced autophosphorylation of PKR, as well as phosphorylation of the PKR substrate eIF2 α (**Fig. 5a** and **Supplementary Fig. 5a**). To determine whether NLRX1 facilitated virus-induced increases in IRF1 protein synthesis by suppressing PKR responses, we generated PH5CH8 cells doubly deficient in NLRX1 and PKR (**Fig. 5b**). The negative effect of the deletion of NLRX1 on SeV-triggered IRF1 responses was completely abolished by PKR deficiency (**Fig. 5c**). PKR deficiency also fully restored the SeV-triggered immediate IL-6 protein response (**Fig. 5d**) and abolished the beneficial effect conferred on HAV replication by NLRX1 deficiency (**Fig. 5e**). We also assessed the effect of SeV infection on nascent protein synthesis in the cells doubly deficient in NLRX1 and PKR. In contrast to the lack of increase in the incorporation of [³⁵S]-Met-Cys or puromycin into NLRX1-deficient cells, relative to that in control PH5CH8 cells (**Fig. 4d,e**), protein synthesis increased over time in response to SeV infection in both cells doubly deficient in NLRX1 and PKR and those deficient in PKR alone (**Fig. 5f** and **Supplementary Fig. 5b**).

To explore the mechanism by which NLRX1 suppressed PKR responses, we investigated whether NLRX1 physically interacted with PKR in hepatocytes. However, no co-immunoprecipitation of PKR protein with either endogenous NLRX1 or overexpressed NLRX1 was detectable in PH5CH8 cells (**Supplementary Fig. 5c,d**). Since NLRX1 binds both viral RNA and poly(I:C), a common surrogate

for viral dsRNA^{27,28}, we reasoned that NLRX1 might suppress the activation of PKR by competing for viral RNA in infected cells. To test our hypothesis, we first confirmed that NLRX1 bound HAV genomic RNA, which is known to have extensive secondary structure²⁹, in bidirectional precipitation assays (**Fig. 5g**). Next, we designed a cell-free competition assay in which lysates of NLRX1-deficient cells were used as a source of PKR, supplemented with purified recombinant NLRX1 protein and biotin-tagged HAV RNA or poly(I:C). The addition of increasing amounts of recombinant NLRX1 protein led to a progressive reduction in the binding of PKR to viral RNA or poly(I:C) (**Fig. 5h**), which indicated that NLRX1 competed with PKR for binding to viral RNA. Together these results demonstrated that NLRX1 suppressed the activation of PKR, in part by competitively binding viral RNA, and thereby prevented the PKR-mediated translational shutdown that would otherwise attenuate IRF1-mediated antiviral responses (**Supplementary Fig. 5e**).

DISCUSSION

Although some studies have reported NLRX1 to be a negative regulator of innate immunity^{3,6,8,30}, others have not confirmed that^{9,31} or have even suggested that NLRX1 enhances antiviral responses¹⁰. Consistent with the latter notion, we found NLRX1 to be an antiviral factor and a positive regulator of early innate immune responses in human hepatocytes. HAV and HCV, both common causes of viral hepatitis in humans, are unrelated, positive-strand hepatotropic RNA viruses that share many similarities in their replication cycles and in their interactions with innate immunity¹². Both produce dsRNA replication intermediates that induce signaling via RIG-I and TLR3 and thereby activate NF- κ B and members of the IRF family, which leads to antiviral defense^{12,32}. To counter those host defenses, both HAV and HCV express proteases that target for degradation MAVS and TRIF, key adaptors in the RIG-I and TLR3 signaling pathways^{33–36}. Adding to those similarities, we found here that NLRX1 acted to restrict the replication of both HAV and HCV.

Surprisingly, we observed that NLRX1 had distinct, opposing effects on the SeV-induced activation of two members of the IRF family. NLRX1 was required for maximal increases in the abundance of IRF1 but suppressed the dimerization of IRF3. As key factors in inducing cytokine transcription, members of the IRF family are triggered by various stimuli in all cell types. Whereas IRF3 and IRF7 are activated by viral infection in most cell types^{37,38}, other family members, including IRF1, as well as IRF5, IRF8 and IRF9, are selectively activated by different stimuli in a cell-type-dependent manner^{39–44}. This complexity in IRF activation provides the diversity of responses required for effective host defense. However, it also allows a single regulatory molecule, such as NLRX1, to have different functional consequences when expressed in different cell types or pathogen contexts or, potentially, at different points of time in the response to an invading virus. The opposing regulatory activities of NLRX1 on early IRF3 and IRF1 responses might account for much of the controversy surrounding this protein^{7,8,10}. We found that NLRX1 positively regulated IRF1 signaling in both BMDMs and primary MEFs. However, NLRX1 is known to attenuate innate immunological control of viral replication in these cell types^{6–8}. We infer from this that IRF1 does not have a dominant role in determining the outcome of infection in these cells, at least not under the conditions tested, whereas our data showed that it did so in hepatocytes. Thus, whether NLRX1 functions as a pro-viral factor or an antiviral factor, or neither^{9,31}, probably reflects which IRFs dominate in inducing antiviral responses.

Although published studies have indicated that NLRX1 negatively regulates lipopolysaccharide- and TLR4-triggered NF- κ B signaling

in macrophages and HEK293T human embryonic kidney cells^{3,7}, we found that NLRX1 had a slight, positive effect on RIG-I-mediated NF- κ B signaling in hepatocytes. However, this effect was not critical for the promotion of early cytokine responses by NLRX1, as our data showed that NLRX1 regulated the IL-6 response downstream of the influence of NF- κ B.

Negative regulation of MAVS-mediated IRF3 responses by NLRX1 has been described previously⁶, but how NLRX1 affects IRF1 responses has not been studied. We found that depleting cells of NLRX1 did not alter SeV-induced transcription of *IRF1* mRNA in PH5CH8 cells, but it significantly reduced the synthesis of IRF1 protein. Reductions in protein synthesis were not specific to IRF1 but instead reflected a global shutdown of protein synthesis due to enhanced activation of PKR, a phenomenon that would probably have its greatest effect on proteins that turn over rapidly, such as IRF1, which has a half-life of about 60 min.

Emerging evidence is increasingly linking translational control to the regulation of immediate responses of the innate immune system. Both IRF7 and IRF8 seem to be controlled via global, regulation of translation dependent on the translation-initiation factor eIF4E^{45–47}. PKR restricts protein synthesis globally by phosphorylating eIF2 α and thereby blocking the production of virus⁴⁸. However, activation of PKR also reduces the synthesis of effector proteins encoded by interferon-stimulated genes⁴⁹ and, as we have shown here, the production of IRF1 driven by an early, NF- κ B-mediated response to SeV. PKR is thus a double-edged sword, potentially weakening the cell's antiviral defenses as well as presenting a hurdle to be overcome by the virus. The negative effect of the activation of PKR on host defense might be particularly important when cells are infected with viruses such as HCV that can continue to translate their RNAs despite such activation⁴⁹. Our data suggest that NLRX1 moderates the potentially negative consequences of PKR activation by competing with it for binding to viral RNA. This is distinct from how other members of the NLR family, including NLRP3, NLRP1 and NLRC4, physically interact with PKR to maximize activation of the inflammasome⁵⁰.

We speculate that the opposing actions of NLRX1 on early IRF1 and IRF3 antiviral responses might underlie much of the controversy surrounding the biological function of this member of the NLR family. Loss of NLRX1 expression might result in contradictory effects on outcome of infections by different viruses in different tissues, depending on which IRF protein dominates in driving the antiviral response.

METHODS

Methods, including statements of data availability and any associated accession codes and references, are available in the online version of the paper.

Note: Any Supplementary Information and Source Data files are available in the online version of the paper.

ACKNOWLEDGMENTS

We thank B. Glaunsinger (University of California, Berkeley) for the human *IL6* 3' UTR expression vector, and L. Hensley, W. Lovell, M. Deng, and M. Chua for technical support. Supported by the US National Institutes of Health (U19-AI109965 to S.M.L., J.A.D. and J.P.-Y.T.; R01-AI103083 to S.M.L.; R01-AI131685 to S.M.L. and J.K.W.; R01-AI103311 to N.J.M.; and R21-AI117575 to J.K.W.) and the University of North Carolina Cancer Research Fund (S.M.L. and J.P.-Y.T.).

AUTHOR CONTRIBUTIONS

H.F. and S.M.L. designed the experiments, analyzed the data and wrote the manuscript; H.F., E.M.L., D.Y., D.R.M., O.G. -L. and I.M. performed experiments; E.W., J.M., H.G., L.M.R., J.K.W., J.P. -Y.T., J.A.D. and N.J.M. provided critical reagents and intellectual input; S.M.L. supervised the study; and all authors reviewed the manuscript.

COMPETING FINANCIAL INTERESTS

The authors declare no competing financial interests.

Reprints and permissions information is available online at <http://www.nature.com/reprints/index.html>. Publisher's note: Springer Nature remains neutral with regard to jurisdictional claims in published maps and institutional affiliations.

1. Guo, H., Callaway, J.B. & Ting, J.P. Inflammasomes: mechanism of action, role in disease, and therapeutics. *Nat. Med.* **21**, 677–687 (2015).
2. Schneider, M. *et al.* The innate immune sensor NLRC3 attenuates Toll-like receptor signaling via modification of the signaling adaptor TRAF6 and transcription factor NF- κ B. *Nat. Immunol.* **13**, 823–831 (2012).
3. Xia, X. *et al.* NLRX1 negatively regulates TLR-induced NF- κ B signaling by targeting TRAF6 and IKK. *Immunity* **34**, 843–853 (2011).
4. Benko, S., Magalhães, J.G., Philpott, D.J. & Girardin, S.E. NLRC5 limits the activation of inflammatory pathways. *J. Immunol.* **185**, 1681–1691 (2010).
5. Allen, I.C. *et al.* NLRP12 suppresses colon inflammation and tumorigenesis through the negative regulation of noncanonical NF- κ B signaling. *Immunity* **36**, 742–754 (2012).
6. Moore, C.B. *et al.* NLRX1 is a regulator of mitochondrial antiviral immunity. *Nature* **451**, 573–577 (2008).
7. Allen, I.C. *et al.* NLRX1 protein attenuates inflammatory responses to infection by interfering with the RIG-I-MAVS and TRAF6-NF- κ B signaling pathways. *Immunity* **34**, 854–865 (2011).
8. Guo, H. *et al.* NLRX1 Sequesters STING to negatively regulate the interferon response, thereby facilitating the replication of HIV-1 and DNA viruses. *Cell Host Microbe* **19**, 515–528 (2016).
9. Rebsamen, M. *et al.* NLRX1/NOD5 deficiency does not affect MAVS signalling. *Cell Death Differ.* **18**, 1387 (2011).
10. Jaworska, J. *et al.* NLRX1 prevents mitochondrial induced apoptosis and enhances macrophage antiviral immunity by interacting with influenza virus PB1-F2 protein. *Proc. Natl. Acad. Sci. USA* **111**, E2110–E2119 (2014).
11. Tattoli, I. *et al.* NLRX1 is a mitochondrial NOD-like receptor that amplifies NF- κ B and JNK pathways by inducing reactive oxygen species production. *EMBO Rep.* **9**, 293–300 (2008).
12. Qu, L. & Lemon, S.M. Hepatitis A and hepatitis C viruses: divergent infection outcomes marked by similarities in induction and evasion of interferon responses. *Semin. Liver Dis.* **30**, 319–332 (2010).
13. Ikeda, M. *et al.* Human hepatocyte clonal cell lines that support persistent replication of hepatitis C virus. *Virus Res.* **56**, 157–167 (1998).
14. Li, K., Chen, Z., Kato, N., Gale, M. Jr. & Lemon, S.M. Distinct poly(I-C) and virus-activated signaling pathways leading to interferon-beta production in hepatocytes. *J. Biol. Chem.* **280**, 16739–16747 (2005).
15. Yamane, D. *et al.* Differential hepatitis C virus RNA target site selection and host factor activities of naturally occurring miR-122 3' variants. *Nucleic Acids Res.* **45**, 4743–4755 (2017).
16. Feng, Z. *et al.* A pathogenic picornavirus acquires an envelope by hijacking cellular membranes. *Nature* **496**, 367–371 (2013).
17. Abdul-Sater, A.A. *et al.* Enhancement of reactive oxygen species production and chlamydial infection by the mitochondrial Nod-like family member NLRX1. *J. Biol. Chem.* **285**, 41637–41645 (2010).
18. Lei, Y. *et al.* The mitochondrial proteins NLRX1 and TUFM form a complex that regulates type I interferon and autophagy. *Immunity* **36**, 933–946 (2012).
19. Soares, F. *et al.* The mitochondrial protein NLRX1 controls the balance between extrinsic and intrinsic apoptosis. *J. Biol. Chem.* **289**, 19317–19330 (2014).
20. Sumpter, R. Jr. *et al.* Regulating intracellular antiviral defense and permissiveness to hepatitis C virus RNA replication through a cellular RNA helicase, RIG-I. *J. Virol.* **79**, 2689–2699 (2005).
21. Masuda, K. *et al.* Arid5a controls IL-6 mRNA stability, which contributes to elevation of IL-6 level in vivo. *Proc. Natl. Acad. Sci. USA* **110**, 9409–9414 (2013).
22. Odendall, C. *et al.* Diverse intracellular pathogens activate type III interferon expression from peroxisomes. *Nat. Immunol.* **15**, 717–726 (2014).
23. Hiscott, J. Triggering the innate antiviral response through IRF-3 activation. *J. Biol. Chem.* **282**, 15325–15329 (2007).
24. Mboko, W.P. *et al.* Interferon regulatory factor 1 restricts gammaherpesvirus replication in primary immune cells. *J. Virol.* **88**, 6993–7004 (2014).
25. Fujita, T., Kimura, Y., Miyamoto, M., Barsoumian, E.L. & Taniguchi, T. Induction of endogenous IFN- α and IFN- β genes by a regulatory transcription factor, IRF-1. *Nature* **337**, 270–272 (1989).
26. Dauber, B. & Wolff, T. Activation of the antiviral kinase PKR and viral countermeasures. *Viruses* **1**, 523–544 (2009).
27. Hong, M., Yoon, S.I. & Wilson, I.A. Structure and functional characterization of the RNA-binding element of the NLRX1 innate immune modulator. *Immunity* **36**, 337–347 (2012).
28. Unger, B.L. *et al.* Nod-like receptor X-1 is required for rhinovirus-induced barrier dysfunction in airway epithelial cells. *J. Virol.* **88**, 3705–3718 (2014).
29. Brown, E.A., Zajac, A.J. & Lemon, S.M. In vitro characterization of an internal ribosomal entry site (IRES) present within the 5' nontranslated region of hepatitis A virus RNA: comparison with the IRES of encephalomyocarditis virus. *J. Virol.* **68**, 1066–1074 (1994).
30. Barouch, D.H. *et al.* Rapid inflammasome activation following mucosal SIV infection of Rhesus monkeys. *Cell* **165**, 656–667 (2016).

31. Soares, F. *et al.* NLRX1 does not inhibit MAVS-dependent antiviral signalling. *Innate Immun.* **19**, 438–448 (2013).
32. Hirai-Yuki, A. *et al.* MAVS-dependent host species range and pathogenicity of human hepatitis A virus. *Science* **353**, 1541–1545 (2016).
33. Yang, Y. *et al.* Disruption of innate immunity due to mitochondrial targeting of a picornaviral protease precursor. *Proc. Natl. Acad. Sci. USA* **104**, 7253–7258 (2007).
34. Qu, L. *et al.* Disruption of TLR3 signaling due to cleavage of TRIF by the hepatitis A virus protease-polymerase processing intermediate, 3CD. *PLoS Pathog.* **7**, e1002169 (2011).
35. Li, K. *et al.* Immune evasion by hepatitis C virus NS3/4A protease-mediated cleavage of the Toll-like receptor 3 adaptor protein TRIF. *Proc. Natl. Acad. Sci. USA* **102**, 2992–2997 (2005).
36. Li, X.D., Sun, L., Seth, R.B., Pineda, G. & Chen, Z.J. Hepatitis C virus protease NS3/4A cleaves mitochondrial antiviral signaling protein off the mitochondria to evade innate immunity. *Proc. Natl. Acad. Sci. USA* **102**, 17717–17722 (2005).
37. Honda, K. & Taniguchi, T. IRFs: master regulators of signalling by Toll-like receptors and cytosolic pattern-recognition receptors. *Nat. Rev. Immunol.* **6**, 644–658 (2006).
38. Ivashkiv, L.B. & Donlin, L.T. Regulation of type I interferon responses. *Nat. Rev. Immunol.* **14**, 36–49 (2014).
39. Tailor, P. *et al.* The feedback phase of type I interferon induction in dendritic cells requires interferon regulatory factor 8. *Immunity* **27**, 228–239 (2007).
40. Li, P. *et al.* IRF8 and IRF3 cooperatively regulate rapid interferon- β induction in human blood monocytes. *Blood* **117**, 2847–2854 (2011).
41. Lazear, H.M. *et al.* IRF-3, IRF-5, and IRF-7 coordinately regulate the type I IFN response in myeloid dendritic cells downstream of MAVS signaling. *PLoS Pathog.* **9**, e1003118 (2013).
42. Weiss, G. *et al.* MyD88 drives the IFN- β response to *Lactobacillus acidophilus* in dendritic cells through a mechanism involving IRF1, IRF3, and IRF7. *J. Immunol.* **189**, 2860–2868 (2012).
43. Ousman, S.S., Wang, J. & Campbell, I.L. Differential regulation of interferon regulatory factor (IRF)-7 and IRF-9 gene expression in the central nervous system during viral infection. *J. Virol.* **79**, 7514–7527 (2005).
44. Scherbik, S.V., Stockman, B.M. & Brinton, M.A. Differential expression of interferon (IFN) regulatory factors and IFN-stimulated genes at early times after West Nile virus infection of mouse embryo fibroblasts. *J. Virol.* **81**, 12005–12018 (2007).
45. Xu, H. *et al.* Notch-RBP-J signaling regulates the transcription factor IRF8 to promote inflammatory macrophage polarization. *Nat. Immunol.* **13**, 642–650 (2012).
46. Colina, R. *et al.* Translational control of the innate immune response through IRF-7. *Nature* **452**, 323–328 (2008).
47. Lee, M.S., Kim, B., Oh, G.T. & Kim, Y.J. OASL1 inhibits translation of the type I interferon-regulating transcription factor IRF7. *Nat. Immunol.* **14**, 346–355 (2013).
48. Elde, N.C., Child, S.J., Geballe, A.P. & Malik, H.S. Protein kinase R reveals an evolutionary model for defeating viral mimicry. *Nature* **457**, 485–489 (2009).
49. Garaigorta, U. & Chisari, F.V. Hepatitis C virus blocks interferon effector function by inducing protein kinase R phosphorylation. *Cell Host Microbe* **6**, 513–522 (2009).
50. Lu, B. *et al.* Novel role of PKR in inflammasome activation and HMGB1 release. *Nature* **488**, 670–674 (2012).

ONLINE METHODS

Reagents and antibodies. Puromycin and blasticidin were from Invitrogen. 3-methyladenine (3-MA), tauroursodeoxycholic acid (TUDCA), N-acetyl-L-cysteine (NAC), ruxolitinib, tofacitinib, cycloheximide and actinomycin-D were from Sigma-Aldrich. PSI-7977 (Sofosbuvir) was from Chemscence. Poly(I:C) (high molecular weight, InvivoGen) was either added to cell culture supernatants at a final concentration of 50 µg/ml or transfected at a concentration of 2 µg/ml.

Antibodies used in this study included the following: antibody to NLRX1 (anti-NLRX1) (1:5,000 dilution; this antibody was described previously⁶); anti-IRF1 (1:1,000 dilution; clone D5E4, #8478), anti-phospho-NF-κB p65 (anti-p-RELA; 1:1,000 dilution; clone 93H1, #3033), anti-NF-κB p65 (anti-RELA; 1:1,000 dilution; clone D14E12, #8242), anti-p50 (1:1,000 dilution; clone 5D10D11, #13681), anti-phospho-IκBα (1:500 dilution; clone 14D4, #2859), anti-IκBα (1:1,000 dilution; clone L35A5, #4814), anti-PKR (1:1,000 dilution; clone D7F7, #12297) and antibody to phosphorylated eIF2α (1:1,000 dilution; clone S51, #9721), all from Cell Signaling; anti-IRF3 (1:500 dilution; clone FL-425, sc-9082), anti-eIF2α (1:500 dilution; clone FL-315, sc-11386) and anti-lamin A/C (1:1,000 dilution; clone N-18, sc-6215), all from Santa Cruz; antibody to phosphorylated PKR (1:1,000 dilution; clone E120, ab32036) and mouse IgG1 (ab18448), both from Abcam; anti-Cardif (anti-MAVS; 1:2,000 dilution; clone AT107, #ALX-210-929), from Enzo Life Sciences; anti-actin (1:40,000 dilution; clone AC-74, A2228), from Sigma; anti-GAPDH (1:50,000 dilution; AM4300), from Ambion; and anti-puromycin (1:20,000 dilution for immunoblot and 1:10,000 dilution for immunofluorescence; clone 12D10, MABE343), from EMD Millipore. Goat anti-mouse IgG (H+L) cross-adsorbed secondary antibody (1:300 dilution; A-11001) was from ThermoFisher. IRDye 680 or 800 secondary antibodies included #926-32211, #926-32212, #926-32214, #926-68020 and #926-68073 (1:12,000) from LI-COR Biosciences.

Cells. Tissues for preparation of fetal human liver cells were from anonymous donors and were provided by the accredited nonprofit corporation Advanced Biosciences Resources (ABR); they were obtained from fetuses between 19 weeks and 21 weeks of gestation during elective termination of pregnancy. Tissues were collected with written informed consent from all donors and in accordance with the US Food and Drug Administration CFR Part 1271 Good Tissue Practices regulations. Tissue processing and hepatoblast isolation and culture were as previously described⁵¹. The use of commercially procured fetal liver cells was reviewed by the University of North Carolina at Chapel Hill Office of Human Research Ethics and was determined to be exempt from review by the University of North Carolina at Chapel Hill Institutional Review Board.

293FT cells and human hepatocyte-derived cell lines, including Huh-7.5 cells⁵² and PH5CH8 cells¹³, were mycoplasma free and were cultured as previously described⁵¹. Mouse bone-marrow-derived macrophages (BMDMs) and mouse embryo fibroblasts (MEFs) were generated and cultured as previously described⁸.

Mice and HAV RNA inoculation. Age- and sex-matched wild-type and *Nlrp1*^{-/-} mice were previously described⁷. Animals were stratified by sex before randomization. Experiments were performed in a non-blinded fashion in accordance with the NIH Guide for the Care and Use of Laboratory Animals and with the approval of the Institutional Animal Care and Use Committee of the University of North Carolina at Chapel Hill. 13-week-old mice were inoculated intravenously with PBS or 15 µg *in vitro*-transcribed HAV RNA in a volume of PBS equivalent to ~5% body weight. Mice were killed 3 h after injection, and liver tissue was collected for analysis of cytokine-encoding mRNA by qRT-PCR.

Virus. Sendai virus (SeV, Cantell strain) was obtained from Charles River Laboratory. Cultures were exposed to SeV at a concentration of 600 HA units/ml. High-titer HAV stock (HM175/18f strain⁵³) was prepared as described previously⁵⁴. HAV infection was carried out at a multiplicity of infection of 10 for PH5CH8 cells or a multiplicity of infection of 1 for Huh-7.5 cells. Infectious molecular clones for HCV (p)FH1-QL, containing the cell-culture-adaptive mutation Q221L in the NS3 helicase⁵⁵, a reporter virus expressing *Gaussia princeps* luciferase (p)FH1-QL/GLuc⁵¹, and HAV (pT7-18f)⁵⁶ were described previously.

Plasmids and oligonucleotides. Firefly luciferase reporter vectors, including pIFNB1-Luc, pIRF3-responsive (4*PRD(I/III))-Luc and pPRDII-Luc, as well as the Renilla luciferase control reporter vector pRL-TK, were described previously⁵⁷. The *IL6* 3'UTR construct was provided by B. Glaunsinger (University of California, Berkeley) and was sub-cloned to psiCHECK2. Plasmids for over-expression of NLRX1 and PKR were previously described⁶. An expression vector for reconstitution of NLRX1 was generated by removal of the TurboGFP-2A region from pLOC-RFP⁵⁸, producing pLOCΔGFP, which retains the RFP open reading frame (ORF) (empty vector, EV). The RFP ORF was then replaced by sequence encoding the NLRX1 ORF to produce pLOC-NLRX1T3, using a PCR-based strategy as previously described⁵⁹. Oligonucleotides used in this study are listed in **Supplementary Table 2**. All constructs were verified by DNA sequencing.

In vitro transcription and transfection. *In vitro* transcription and transfection of viral RNA was performed as previously described⁵¹. For biotin labeling of HAV RNA, transcription mixes were supplemented with 1× concentrated Biotin RNA Labeling Mix (Roche). siLentfect Lipid Reagent (Bio-Rad) was used for transfection of siRNA (*NLRX1* 5'-AUCCCGACGGAAGAUGUGC-3' and control #2, both from Dharmacon; *NFKB1* from Santa Cruz). Fugen HD Reagent (Promega) was used for DNA transfections.

Lentivirus production and transduction. For sgRNA CRISPR-Cas9 lentivirus production, individual sgRNA expressing vectors and the 3rd Generation Packaging Mix vectors (ABM) were co-transfected into 293FT cells. Transduction was facilitated by the addition of 8 µg/ml polybrene, and the resulting cells were subjected to selection with puromycin (6 µg/ml) for single-deletion cells, and puromycin (6 µg/ml) and blasticidin (10 µg/ml) for double-deletion cells.

RNA extraction and quantitative RT-PCR. Total RNA extraction was carried out with the RNeasy Kit (Qiagen), followed by two-step quantitative RT-PCR analysis of genes with the SuperScript III First-Strand Synthesis System (Invitrogen) and iTaq SYBR Green Supermix (Bio-Rad). The abundance of indicated genes was normalized to that of *ACTB* (human) or *Actb* (mouse). The abundance of HAV and HCV RNA was quantified as previously described^{51,60}.

Nuclear protein extraction. Extraction of nuclear proteins was carried out as previously described⁶¹, with minor modification. In brief, the washed nuclei pellet was re-suspended in 50 µl of nuclear protein extraction buffer (20 mM Tris-HCl, pH 7.5, 400 mM NaCl, 1.5 mM MgCl₂ and 0.2 mM EDTA) supplemented with complete protease inhibitor and PhoSTOP (Roche).

Protein-protein-RNA interaction. Cell lysates were prepared from 10-cm dish cultures (1.5 × 10⁶ to 2 × 10⁶ cells) with lysis buffer (20 mM Tris-HCl, pH 7.5, 50 mM KCl, 250 mM NaCl, 10% glycerol, 5 mM EDTA, 1× complete protease inhibitor and 1× PhoSTOP) supplemented with detergents as follows. For protein-protein interaction assays, 0.2% Triton X-100 and 0.3% NP-40 were added. The resulting lysates were used for immunoprecipitation as previously described⁶². For protein-RNA interaction, 0.5% Triton X-100 with 0.1% NP-40 was added. Recombinant NLRX1 was generated as previously described⁶³. Lysates were mixed with an equal volume of 2× incubation buffer (300 mM KCl, 40 mM HEPES, pH 7.5, 10% glycerol, 200 Units/ml RNaseOUT (Thermo Fisher), 10 mM magnesium acetate and 2 mM DTT). For precipitation, 500 ng biotin-labeled HAV RNA, 100 ng biotin-labeled poly(I:C) (InvivoGen) or 1 µl polyclonal anti-NLRX1 was used in each reaction. All reactions were gently rotated at 4 °C for 2 h, followed by the addition of magnetic streptavidin T1 beads (Invitrogen) for another 30 min of rotation or protein G-Sepharose (GE Healthcare) for another 1 h of rotation. After five intense washes with 1× incubation buffer, the final product was analyzed by qRT-PCR and/or immunoblot.

Electrophoretic mobility-shift assay, native PAGE, immunoblot analysis and visualization. For electrophoretic mobility-shift assays, IRDye 700-labeled oligonucleotides containing a consensus NF-κB-binding site (5'-AGTTGAGGGGACTTCCAGGC-3'; LI-COR Biosciences) were incubated

with nuclear extracts according to the manufacturer's protocol (Odyssey Infrared EMSA kit). Electrophoresis of the resultant products was carried out with a 5% TBE gel (Bio-Rad). Native PAGE for analysis of IRF3 dimerization was performed as previously described⁶⁴. Immunoblot analysis was carried out using standard methods. An Odyssey Imaging System (Li-COR Biosciences) was used for visualization and signal (infrared fluorescence) intensity analysis.

Polysome profiling, [³⁵S]-metabolic labeling, and puromycin incorporation assay. Control PH5CH8 cells and PH5CH8 cells depleted of NLRX1 (2×10^7) were infected with SeV (3×10^4 HA units) for 2 h. Cells were then harvested, and polysome gradients were prepared and analyzed as previously described⁶⁵. For metabolic labeling, 3×10^5 cells were infected with SeV (1.5×10^3 HA units) for 2 h and 15 min. After 15 min of starvation in methionine- and cysteine-free medium, newly synthesized proteins were pulse-labeled with [³⁵S]-labeled methionine and cysteine, 125 μ Ci [³⁵S]/ml, for 30 min as described⁶⁶. Protein synthesis was assessed in cells infected by SeV under similar conditions by monitoring of the incorporation of puromycin into nascent protein using a method described previously⁶⁷. In brief, cells grown on glass slides were pulsed with puromycin (10 μ g/ml) for 10 min, then were fixed with 4% paraformaldehyde, followed by staining with anti-puromycin and DAPI. Slides were imaged by laser-scanning confocal microscopy at a fixed gain in an Olympus FV1000 instrument at 40 \times magnification, and recorded images were analyzed with ImageJ (Fiji). Individual cells were identified by DAPI staining of nuclei, and were assigned scores for the intensity of the puromycin signal greater than an arbitrary threshold set with mock-infected control cells in each experiment. Alternatively, cells were lysed, and puromycin-labeled proteins were identified by immunoblot analysis and quantified by assessing infrared fluorescence intensity with the Odyssey Imaging System.

Luciferase reporter assay. Luciferase assays, including secreted *Gaussia* luciferase (GLuc) analysis of HCV replication and dual luciferase assays to analyze promoter activation, were carried out as described previously^{57,68}.

ELISA. IL-6 concentrations were determined with the human IL-6 ELISA Kit (eBioscience) according to the manufacturer's protocol.

Statistical analysis. Unless noted otherwise, all between-group comparisons were carried out by one-way or two-way ANOVA or two-sided *t*-test. Calculations were made using Prism 6.0 software (GraphPad Software).

A **Life Sciences Reporting Summary** for this paper is available. Detailed information about experimental design and reagents used in this study can be found in that summary.

Data availability. Data that support the findings of this study are shown directly in figures accompanying the main text or in supplementary figures or are available from the corresponding author upon request.

51. Yamane, D. *et al.* Regulation of the hepatitis C virus RNA replicase by endogenous lipid peroxidation. *Nat. Med.* **20**, 927–935 (2014).
52. Blight, K.J., McKeating, J.A. & Rice, C.M. Highly permissive cell lines for subgenomic and genomic hepatitis C virus RNA replication. *J. Virol.* **76**, 13001–13014 (2002).
53. Lemon, S.M. *et al.* Antigenic and genetic variation in cytopathic hepatitis A virus variants arising during persistent infection: evidence for genetic recombination. *J. Virol.* **65**, 2056–2065 (1991).
54. Feng, Z. *et al.* Human pDCs preferentially sense enveloped hepatitis A viruses. *J. Clin. Invest.* **125**, 169–176 (2015).
55. Shimakami, T. *et al.* Protease inhibitor-resistant hepatitis C virus mutants with reduced fitness from impaired production of infectious virus. *Gastroenterology* **140**, 667–675 (2011).
56. Yi, M. & Lemon, S.M. Replication of subgenomic hepatitis A virus RNAs expressing firefly luciferase is enhanced by mutations associated with adaptation of virus to growth in cultured cells. *J. Virol.* **76**, 1171–1180 (2002).
57. Dansako, H. *et al.* Class A scavenger receptor 1 (MSR1) restricts hepatitis C virus replication by mediating toll-like receptor 3 recognition of viral RNAs produced in neighboring cells. *PLoS Pathog.* **9**, e1003345 (2013).
58. Saeed, M. *et al.* SEC14L2 enables pan-genotype HCV replication in cell culture. *Nature* **524**, 471–475 (2015).
59. Bryksin, A.V. & Matsumura, I. Overlap extension PCR cloning: a simple and reliable way to create recombinant plasmids. *Biotechniques* **48**, 463–465 (2010).
60. Lanford, R.E. *et al.* Acute hepatitis A virus infection is associated with a limited type I interferon response and persistence of intrahepatic viral RNA. *Proc. Natl. Acad. Sci. USA* **108**, 11223–11228 (2011).
61. Suzuki, K., Bose, P., Leong-Quong, R.Y., Fujita, D.J. & Riabowol, K. REAP: A two minute cell fractionation method. *BMC Res. Notes* **3**, 294 (2010).
62. Li, Y., Masaki, T., Shimakami, T. & Lemon, S.M. hnRNP L and NF90 interact with hepatitis C virus 5'-terminal untranslated RNA and promote efficient replication. *J. Virol.* **88**, 7199–7209 (2014).
63. Mo, J. *et al.* Pathogen sensing by nucleotide-binding oligomerization domain-containing protein 2 (NOD2) is mediated by direct binding to muramyl dipeptide and ATP. *J. Biol. Chem.* **287**, 23057–23067 (2012).
64. Wang, Q. *et al.* Role of double-stranded RNA pattern recognition receptors in rhinovirus-induced airway epithelial cell responses. *J. Immunol.* **183**, 6989–6997 (2009).
65. Masaki, T. *et al.* miR-122 stimulates hepatitis C virus RNA synthesis by altering the balance of viral RNAs engaged in replication versus translation. *Cell Host Microbe* **17**, 217–228 (2015).
66. Ziehr, B., Vincent, H.A. & Moorman, N.J. Human cytomegalovirus pTRS1 and pIRS1 antagonize protein kinase R to facilitate virus replication. *J. Virol.* **90**, 3839–3848 (2016).
67. Schmidt, E.K., Clavarino, G., Ceppi, M. & Pierre, P. SUNSET, a nonradioactive method to monitor protein synthesis. *Nat. Methods* **6**, 275–277 (2009).
68. Shimakami, T. *et al.* Stabilization of hepatitis C virus RNA by an Ago2-miR-122 complex. *Proc. Natl. Acad. Sci. USA* **109**, 941–946 (2012).